



Microstructure and mechanical properties of ceramic coatings formed on 6063 aluminium alloy by micro-arc oxidation

Nan XIANG^{1,2}, Ren-guo SONG^{1,2}, Jian ZHAO^{1,2}, Hai LI^{1,2}, Chao WANG^{1,2}, Zhi-xiu WANG^{1,2}

1. School of Materials Science and Engineering, Changzhou University, Changzhou 213164, China;

2. Jiangsu Key Laboratory of Materials Surface Science and Technology,
Changzhou University, Changzhou 213164, China

Received 14 November 2014; accepted 25 March 2015

Abstract: The microstructure and mechanical properties of ceramic coatings formed on 6063 aluminium alloy obtained in silicate-, borate- and aluminate-based electrolyte without and with nanoadditive Al_2O_3 and TiO_2 by micro-arc oxidation (MAO) were studied by scanning electron microscopy (SEM), energy-dispersive X-ray spectroscopy (EDS), X-ray diffraction (XRD), microhardness and friction–abrasion tests, respectively. SEM results show that coatings with nanoadditive have less porosities than those without nanoadditive. XRD results reveal that nanoadditive-containing coatings contain more oxides compared with nanoadditive-free coatings in all cases, which are consistent with the EDS analysis. Mechanical properties tests show that nanoadditive Al_2O_3 -containing coatings have higher microhardness values compared with the other coatings obtained in silicate-, borate- and aluminate-based electrolyte. On the other hand, nanoadditive has a positive effect on improving the wearing-resistance of MAO coatings in all cases. Furthermore, the borate-MAO coatings present an inferior anti-wearing property compared with the silicate- and aluminate-MAO coatings for both the nanoadditive-free and nanoadditive-containing coatings.

Key words: 6063 aluminium alloy; micro-arc oxidation; microstructure; mechanical properties; nanoadditive

1 Introduction

Aluminium alloys are widely used in aerospace and automotive industry because of their excellent properties such as high strength, low density, non-magnetic properties and good formability [1,2]. However, the poor surface hardness and wear resistance limited their application in many ways [3]. Various applications had been attempted to overcome its weakness, one of the effective ways to improve their mechanical properties is the surface modification by protecting coatings, which prevent the direct contact from our environment [4–6]. Among them, micro-arc oxidation (MAO) has been widely studied in recent years as an emerging environmentally friendly technology for preparing ceramic coatings on valve metals (such as Al, Mg and Ti) to restrict the directly contact with our environment [7–9].

The MAO process was extremely complicated and involved many influencing factors [10], which consisted of electrical breakdown voltage, electrolyte composition,

the nature of the material itself, effects of additive incorporation and some processing parameters, like current density [11–14]. In our previous work, the 6063 aluminium alloy MAO coatings were obtained in nanoadditive-free and nanoadditive-containing electrolytes [15] and the influence of concentrations of nanoadditive TiO_2 -containing electrolyte on MAO coatings was studied [16], but the influence among different main-electrolytes without or with different nanoadditive on aluminium alloys was not studied.

In the present study, the ceramic coatings were prepared on 6063 aluminium alloy by MAO technique with silicate-, borate- and aluminate-based electrolyte without or with nanoadditive Al_2O_3 and TiO_2 , respectively. The aim of the study was to systematically investigate the microstructure, hardness and friction–abrasion properties of coatings and compare the difference among them.

2 Experimental

The substrate material in the present study was 6063

aluminium alloy (0.45%–0.90% Mg, 0.35% Fe, 0.2%–0.6% Si, 0.10% Cu, 0.10% Mn, 0.10% Cr, 0.10% Zn, 0.10% Ti and balance Al, mass fraction) for MAO experiment. The commercial samples of 6063 aluminium alloy (30 mm × 25 mm × 3 mm) were ground by alumina waterproof abrasive paper up to 1800 grit and ultrasonically cleaned in pure ethanol for degreasing, and then cleaned by distilled water and dried in air. The MAO treatment was carried out using a pulsed AC power source in alkaline silicate-, borate-, aluminate-based electrolyte, respectively. Three types of electrolytes were composed of 10 g/L sodium silicate (Na_2SiO_3), 10 g/L sodium borate ($\text{Na}_2\text{B}_4\text{O}_7$), 10 g/L sodium aluminate (NaAlO_2) and 3 g/L KOH in distilled water, respectively. The nanoadditives were 3.2 g/L titania (TiO_2) and 3.2 g/L alumina (Al_2O_3) for each main-electrolyte, respectively. All the nanoadditives were with a size of about 10 nm and dispersed in solution evenly. Coatings were obtained at a current density of 15 A/dm² for 60 min in all electrolytes. The treatment temperature was always kept at (28±2) °C by a recyclable water cooling system. All the specimens were rinsed thoroughly with distilled water and dried in air immediately after the treatment.

The surface morphologies of coatings were observed by scanning electron microscopy (SEM, Hitachi S-4700) with amplifying magnitude. The semi-quantitative chemical compositions of all coatings were analyzed by energy-dispersive X-ray spectroscopy

(EDS) incorporated into scanning electron microscopy after Au deposition by sputtering. The scanning method was flat scanning with a duplication of three times for the reliability. The phase compositions of the MAO coatings were analyzed by X-ray diffraction (XRD, Thermo ARL X' TRA) using Cu K_α radiation at 2θ values between 25° and 75° with a step length of 0.02° at a scanning rate of 1 (°)/min. The hardness values of the coatings were evaluated by using an HMV-IT Vickers microhardness tester under a load of 200 g. The tribological properties of the coatings were performed on a WTM-2E ball-on-disk tribometer with a rotational speed of 336 r/min. The coating served as the disc, and the counterpart was Si_3N_4 ceramic ball (4 mm in diameter, HV 1550 in hardness). The abrasion loss was measured after 1 h friction measurement with an electronic direct reading balance (LJBROR L-200, readability 0.01 mg).

3 Results and discussion

Based on the main-electrolyte, the coatings prepared in silicate-, aluminate- and borate-based MAO coating are addressed as Si-, Al- and B-MAO coatings in the later discussion.

3.1 SEM observation and EDS analysis

Figure 1 demonstrates the evolution of surface

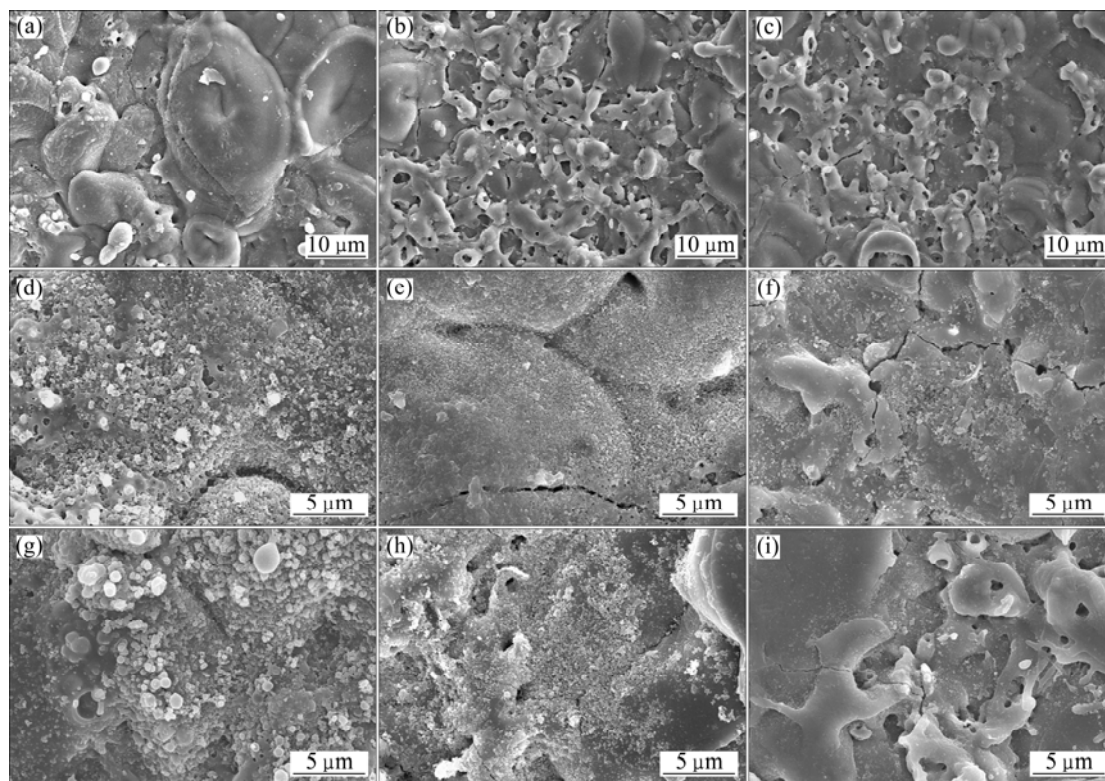


Fig. 1 Morphologies of MAO coatings without nanoadditive (a–c), with nanoadditive TiO_2 (d–f), with nanoadditive Al_2O_3 (g–i) prepared in silicate- (a, d, g), borate- (b, e, h) and aluminate-based (c, f, i) alkaline electrolytes

morphology of MAO coatings. The MAO coatings prepared under electrolytes without nanoadditive (Fig. 1(a)–(c)) presented different images among them. The Si-based MAO coating was of marginal micropores compared with the B- and Al-based coatings. On the other hand, micro-cracks caused by non-homogeneous distribution of thermal stress during MAO process presented on the coatings. Lots of alumina was melted on Si-MAO coating. The Al-MAO coating was smoother and only with little fusing alumina on its surface. The B-MAO coating was more porous compared with other two coatings. The final voltages of Si-, B-, and Al-MAO coatings were 510, 540, 480 V respectively, which may be the direct reason connected to the difference between the surface morphologies. The surface images of MAO coatings with nanoadditive TiO_2 and Al_2O_3 are shown in Figs. 1(d)–(f) and Figs. 1(g)–(i), respectively. It can be seen that the Si-MAO and B-MAO coatings with nanoadditive had less pores on surfaces compared with the Al-MAO coating with nanoadditive. This indicated that nanoparticles introduced into electrolyte could embed in the discharge channels by diffusion and electrophoresis during the MAO process [17]. The Al-MAO coating with nanoadditive exhibited relatively high porosity compared with the other two. There were some differences between the nanoadditive TiO_2 - and Al_2O_3 -containing Al-MAO coatings. The TiO_2 -containing Al-MAO coating had more micro-cracks while there were more pores for the Al_2O_3 -containing Al-MAO coatings. So, all the nanoadditive-containing MAO coatings had much less defects compared with the nanoadditive-free coatings with porosity and microcracks. In general, the nanoadditive decreased the defects of MAO coatings on the surface in all cases.

Figure 2 represents the EDS spectra of the MAO coatings fabricated in electrolytes without nanoadditive. It can be found that the main elements Al and O existed in all coatings. Furthermore, the Si-MAO and B-MAO coatings had more elements compared with the Al-MAO coating. From Figs. 3(a)–(c), it can be seen that the nanoadditive-free and both nanoadditive-containing Al-MAO coatings contained more aluminium than other coatings. This indicated that some aluminum elements in sodium aluminate here were oxidized into alumina, which accorded with the EDS spectrum in Fig. 2(c). On the other hand, Ti content of the nanoadditive TiO_2 -containing MAO coating prepared under Al-based electrolyte was twice lower than that of the B-MAO one and lower than that of the Si-MAO one, either, which can be inferred that only a few TiO_2 nanoparticles were sintered into the coating. This also testified the defective morphology of TiO_2 -containing Al-MAO coating. All the histograms in Fig. 3 showed that the oxygen-containing nanoadditive MAO coatings had more oxide compared

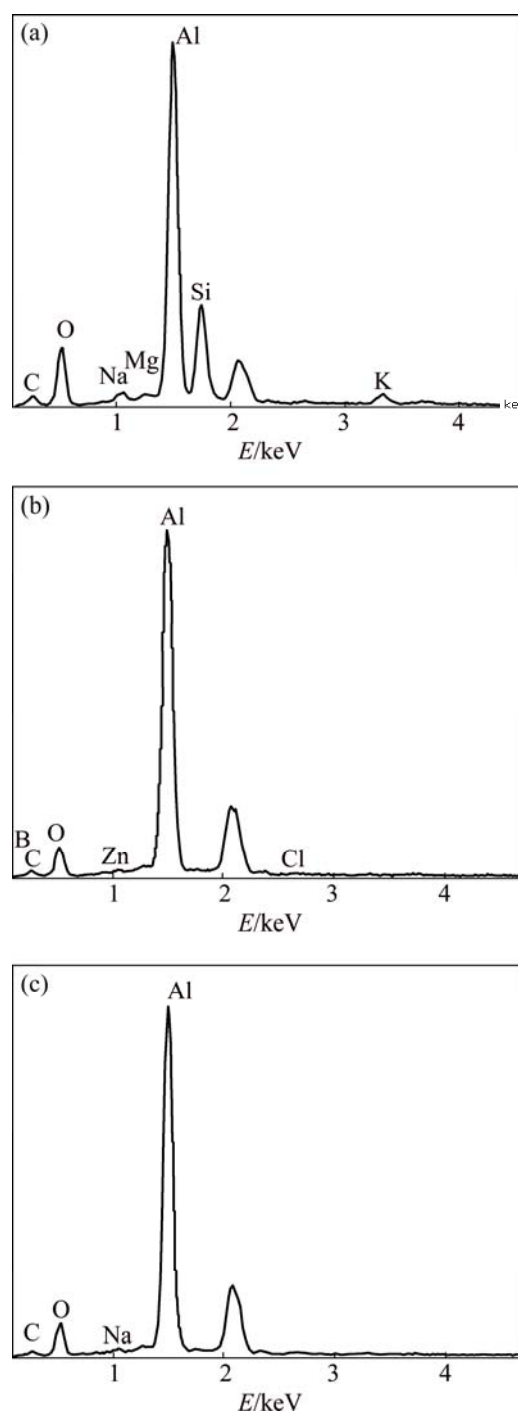


Fig. 2 EDS spectra of Si- (a), B- (b), Al-MAO (c) coating without nanoadditive

with the nanoadditive-free MAO coatings, which matched well with the hypothesis on surface morphologies, that is, the nanoparticles can be sintered into the discharge channels and micropores in MAO process.

3.2 Phase analysis

XRD analyses of MAO coatings with or without nanoadditive are shown in Fig. 4. Two crystal phases

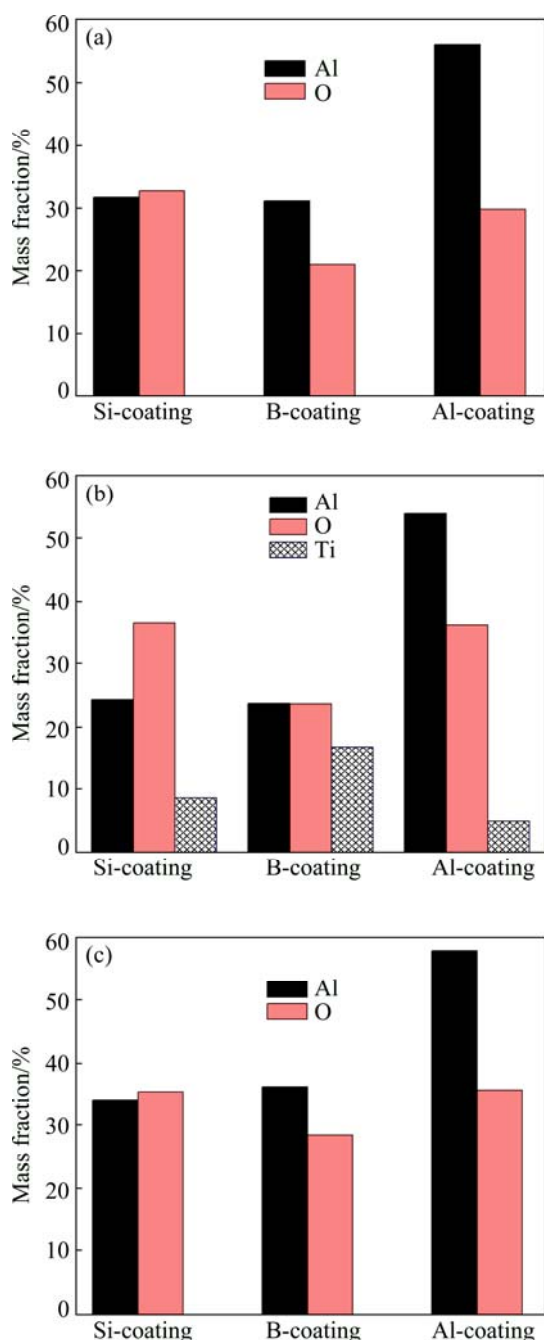


Fig. 3 Elemental contents of MAO coatings without nanoadditive (a), with nanoadditive TiO_2 (b) and nanoadditive Al_2O_3 (c)

$\alpha\text{-Al}_2\text{O}_3$ and $\gamma\text{-Al}_2\text{O}_3$ were detected for both the nanoadditive-free and nanoadditive-containing MAO coatings. The nanoadditive-containing MAO coatings (Figs. 4(b)–(c)) showed higher oxide contents compared with the nanoadditive-free MAO coatings (Fig. 4(a)). On the other hand, the detection of TiO_2 -containing MAO coatings revealed more crystal phases TiO_2 and Ti_3O_5 significantly other than alumina phases. In addition, a few peaks corresponding to AlTi were detected. These results indicated that the constituents of titanium dioxide from the electrolyte participated in the plasma thermo-

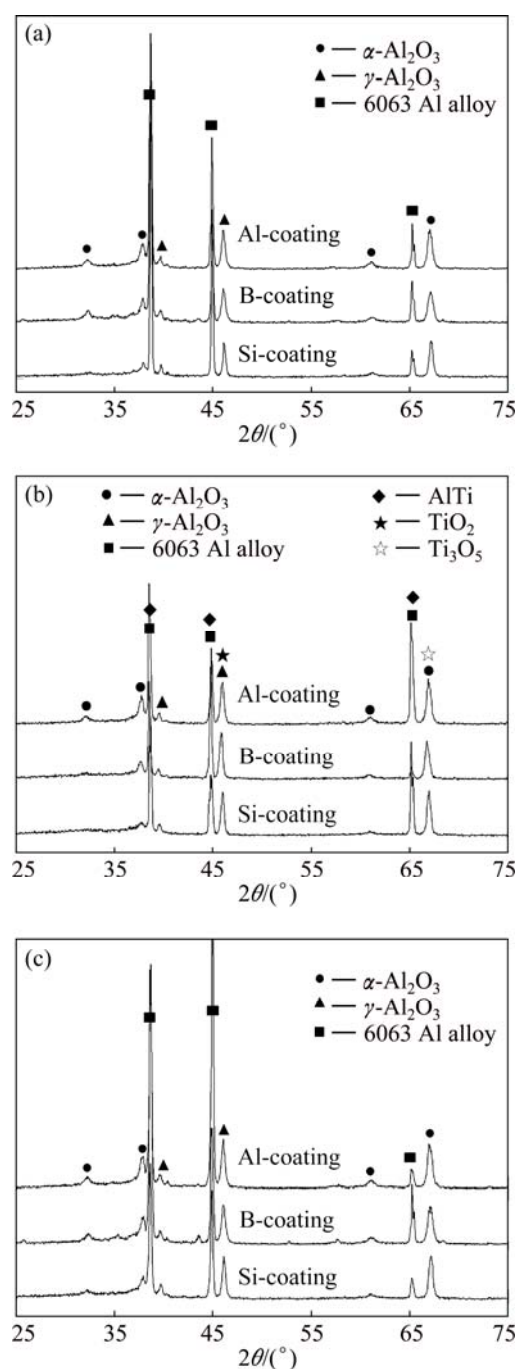


Fig. 4 XRD patterns of MAO coatings prepared under nanoadditive-free (a), nanoadditive TiO_2 -containing (b) and Al_2O_3 -containing (c) conditions

chemical reactions during the MAO process and were incorporated into the coating as compounds. For all MAO coatings, the diffraction peaks of Al corresponding to the substrate were detected.

3.3 Mechanical properties of MAO coatings

The microhardness tests were carried out on specimen obtained in all conditions, and the results are shown in Table 1. Four random points were taken to get a mean value for error reduction in microhardness value.

The coatings obtained at the same level with or without different nanoadditives were on the same standard, respectively. The coatings prepared with nanoadditive-containing electrolytes had much higher microhardness values compared with the nanoadditive-free coatings in general. Furthermore, the microhardness of the MAO coatings prepared with Al_2O_3 -containing electrolyte was improved by nearly 40% compared with that of the nanoadditive-free coatings, which was also 20 % higher than that of MAO coatings with nanoadditive TiO_2 . Such a considerable increase in hardness was attributed to better crystallization and surface morphology with few defects comparably. Therefore, it can be concluded that the nanoadditive is beneficial to improving the microhardness of MAO coatings.

Table 1 Average microhardnesses of ceramic coatings prepared in silicate, borate and aluminate-based electrolytes without nanoadditive and with nanoadditives of TiO_2 and Al_2O_3 , respectively

Nanoadditive	Hardness (HV)		
	Si-coating	B-coating	Al-coating
No	1350	1312	1325
TiO_2	1610	1600	1520
Al_2O_3	1865	1850	1840

The friction coefficients of Si-, B- and Al-MAO coatings without nanoadditive are shown in Fig. 5. From Fig. 5, it could be seen that friction coefficient of the B-MAO coating had an obvious shift during the test. The mass loss of nanoadditive-free B-MAO coating was significantly more than that of the others in Table 2, which indicated that the B-coating was worn out. Besides, the coefficient curves for Si- and Al-MAO coatings without nanoadditive only had a marginal drop and were more inerratic compared with that of the B-MAO coating, which meant that the wearing resistances of Si- and

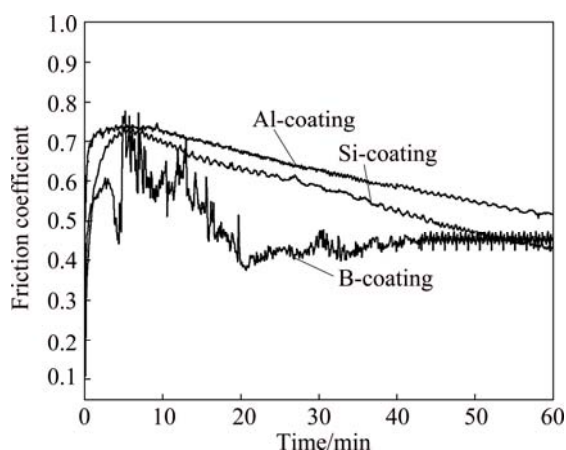


Fig. 5 Friction coefficients of Si-, B- and Al-MAO coatings without nanoadditive

Al-MAO coatings were superior to that of the B-MAO coating. On the other hand, the mass loss of the nanoadditive-containing MAO coatings was less than that of the nanoadditive-free MAO coating in Table 2, and there was a decline in Al_2O_3 -containing coatings and TiO_2 -containing coatings, especially for the B-based MAO coatings. This indicated that the Al_2O_3 -containing MAO coatings had a more positive effect on the anti-wearing property compared with the TiO_2 -containing MAO coatings. On the whole, the nanoadditive could promote the wearing resistance for MAO coatings, which was mainly attributed to the dense surface and high hardness.

Table 2 Mass loss of Si-, B- and Al-MAO coatings without nanoadditive or with nanoadditives of Al_2O_3 and TiO_2 , respectively

Nanoadditive	Mass fraction/%		
	Si-coating	B-coating	Al-coating
No	0.22	3.07	0.18
TiO_2	0.18	1.76	0.13
Al_2O_3	0.15	1.53	0.05

4 Conclusions

1) Micro-arc oxidation coatings were prepared on 6063 aluminium alloy in silicate, borate and aluminate-based electrolytes without or with different nanoadditives, and the effects of electrolyte without or with different nanoadditives on the microstructure and mechanical properties were thoroughly discussed.

2) The nanoadditive can improve the mechanical properties and embed the surface defects of MAO coatings in all cases generally. The TiO_2 -containing MAO coatings have more crystal phases than the $\alpha\text{-Al}_2\text{O}_3$ - and $\gamma\text{-Al}_2\text{O}_3$ -containing MAO coatings. The nanoadditive-containing B-MAO coatings have more different morphologies compared with the others.

3) The B-MAO coatings are inferior in hardness and anti-wearing properties compared with the Al-MAO coatings for both nanoadditive-free and nanoadditive-containing coatings. The Al-MAO coatings with nanoadditive Al_2O_3 show the best mechanical properties in microhardness and wearing resistance compared with the others.

References

- [1] WEN Lei, WANG Ya-ming, ZHOU Yu, OUYANG Jia-hu, GUO Li-xin, JIA De-chang. Corrosion evaluation of microarc oxidation coatings formed on 2024 aluminium alloy [J]. Corrosion Science, 2010, 52: 2687–2696.
- [2] DING H Y, DAI Z D, SKUIRY S C, HUI D. Corrosion wear behaviors of micro-arc oxidation coating of Al_2O_3 on 2024Al in

- different aqueous environments at fretting contact [J]. Tribology International, 2010, 43: 868–875.
- [3] MALAYOGLU U, TEKIN K C, SHRESTHA S. An investigation into the mechanical and tribological properties of plasma electrolytic oxidation and hard-anodized coatings on 6082 aluminum alloy [J]. Material Science and Engineering A, 2011, 528: 7451–7460.
- [4] JAVIDI M, FADAEE H. Plasma electrolytic oxidation of 2024-T3 aluminum alloy and investigation on microstructure and wear behavior [J]. Applied Surface Science, 2013, 286: 212–219.
- [5] LI Qing-biao, LIANG Jun, LIU Bai-xing, PENG Zhen-jun, WANG Qing. Effects of cathodic voltages on structure and wear resistance of plasma electrolytic oxidation coatings formed on aluminium alloy [J]. Applied Surface Science, 2014, 297: 176–181.
- [6] SONG Ren-guo, WANG Chao, JIANG Yan, LI Hai, LU Guo, WANG Zhi-xiu. Microstructure and properties of $\text{Al}_2\text{O}_3/\text{TiO}_2$ nanostructured ceramic composite coatings prepared by plasma spraying [J]. Journal of Alloys and Compounds, 2012, 544: 13–18.
- [7] GAO Hai-tao, ZHANG Meng, YANG Xin, HUANG Ping, XU Ke-wei. Effect of Na_2SiO_3 solution concentration of micro-arc oxidation process on lap-shear strength of adhesive-bonded magnesium alloys [J]. Applied Surface Science, 2014, 314: 447–452.
- [8] ERARSLAN Y. Wear performance of in-situ aluminum matrix composite after micro-arc oxidation [J]. Transactions of Nonferrous Metals Society of China, 2013, 23(2): 347–352.
- [9] LI H X, RUDNEV V S, ZHENG X H, YAROVAYA T P, SONG R G. Characterization of Al_2O_3 ceramic coatings on 6063 aluminum alloy prepared in borate electrolytes by micro-arc oxidation [J]. Journal of Alloys and Compounds, 2008, 462: 99–102.
- [10] YANG Guang-liang, LÜ Xian-yi, BAI Yi-zhen, CUI Hai-feng, JIN Zeng-sun. The effects of current density on the phase composition and microstructure properties of micro-arc oxidation coatings [J]. Journal of Alloys and Compounds, 2002, 345: 196–200.
- [11] ZHOU Fei, WANG Yuan, DING Hong-yan, WANG Mei-ling, YU Min, DAI Zhen-dong. Friction characteristic of micro-arc oxidative Al_2O_3 coatings sliding against Si_3N_4 balls in various environments [J]. Surface and Coatings Technology, 2008, 202: 3808–3814.
- [12] YAN Yuan-yuan, HAN Yong, LI Di-chen, HUANG Juan-juan, LIAN Qin. Effect of NaAlO_2 concentrations on microstructure and corrosion resistance of $\text{Al}_2\text{O}_3/\text{ZrO}_2$ coatings formed on zirconium by micro-arc oxidation [J]. Applied Surface Science, 2010, 256: 6359–6366.
- [13] CAI Jing-shun, CAO Fa-he, CHANG Lin-rong, ZHENG Jun-jun, ZHANG Jian-qing, CAO Chu-nan. The preparation and corrosion behaviors of MAO coating on AZ91D with rare earth conversion precursor film [J]. Applied Surface Science, 2011, 257: 3804–3811.
- [14] YANG Yue, WU Hua. Effect of current density on corrosion resistance of micro-arc oxide coatings on magnesium alloy [J]. Transactions of Nonferrous Metals Society of China, 2010, 20(S2): s688–s692.
- [15] LI Hong-xia, LI Wei-jie, SONG Ren-guo, JI Zheng-guo. Effects of different current densities on properties of MAO coatings embedded with and without $\alpha\text{-Al}_2\text{O}_3$ nanoadditives [J]. Materials Science and Technology, 2012, 28: 565–568.
- [16] LI Hong-xia, SONG Ren-guo, JI Zheng-guo. Effects of nanoadditive TiO_2 on performance of micro-arc oxidation coatings formed on 6063 aluminum alloy [J]. Transactions of Nonferrous Metals Society of China, 2013, 23(2): 406–411.
- [17] YANG Yue, LIU Yao-hui. Effects of current density on the microstructure and the corrosion resistance of alumina coatings embedded with SiC nano-particles produced by micro-arc oxidation [J]. Journal of Materials Science and Technology, 2010, 26: 1016–1020.

6063 铝合金微弧氧化陶瓷涂层的显微组织和力学性能

项南^{1,2}, 宋仁国^{1,2}, 赵坚^{1,2}, 李海^{1,2}, 王超^{1,2}, 王芝秀^{1,2}

1. 常州大学 材料科学与工程学院, 常州 213164;

2. 常州大学 江苏省材料表面科学与技术重点实验室, 常州 213164

摘要: 以硅酸盐、硼酸盐和铝酸盐为主要溶液, 分别在这3种溶液中添加纳米添加剂 Al_2O_3 和 TiO_2 以及不添加纳米添加剂, 制备 6063 铝合金的微弧氧化陶瓷涂层。利用扫描电镜(SEM)、电子能谱分析(EDS)、X 射线衍射、硬度和摩擦磨损测试研究这些涂层的显微组织和力学性能。SEM 结果显示, 含纳米添加剂涂层的孔洞比不含添加剂涂层的孔洞少。X 射线衍射结果表明, 在每种溶液中含添加剂的涂层比不含添加剂的涂层含有更多的氧化物成分, 这与 EDS 的分析结果是一致的。力学性能测试结果表明, 含纳米添加剂 Al_2O_3 的涂层较其他各种情况下在硅酸盐、硼酸盐和铝酸盐中制备出的涂层具有更高的硬度; 纳米添加剂在这3种溶液中都能够提高微弧氧化涂层的耐磨性能。此外, 无论是否含有纳米添加剂, 硼酸盐微弧氧化涂层相对于硅酸盐和铝酸盐涂层都表现出较差的耐磨性能。

关键词: 6063 铝合金; 微弧氧化; 显微组织; 力学性能; 纳米添加剂

(Edited by Wei-ping CHEN)